



 Cite this: *RSC Adv.*, 2022, 12, 2751

Mechanistic studies of visible light-induced CO release from a 3-hydroxybenzo[g]quinolone†

 Marina Popova,^a Tomasz Borowski,^b *^b Josiah G. D. Elsberg,^b ^a C. Taylor Dederich^a and Lisa M. Berreau *^a

Organic compounds that can be triggered using light to release CO in biological environments are of significant current interest to probe the role of CO in biology and as potential therapeutics. We recently reported that a 3-hydroxybenzo[g]quinolone (**5**) can be used as a CO delivery molecule to produce anticancer and potent anti-inflammatory effects. Herein we report mechanistic studies of the visible light-induced CO release reaction of this compound. In wet CH₃CN under aerobic conditions, **5** releases 0.90(2) equivalents of CO upon illumination with visible light (419 nm) to give a single depside product. Performing the same reaction under an ¹⁸O₂ atmosphere results in quantitative incorporation of two labeled oxygen atoms in the depside product. Monitoring *via* ¹H NMR and UV-vis during the illumination of **5** in CH₃CN using 419 nm light revealed the substoichiometric formation of a diketone (**6**) in the reaction mixture. H₂O₂ formation was detected in the same reaction mixtures. DFT studies indicate that upon light absorption an efficient pathway exists for the formation of a triplet excited state species (**5b**) that can undergo reaction with ³O₂ resulting in CO release. DFT investigations also provide insight into diketone (**6**) and H₂O₂ formation and subsequent reactivity. The presence of water and exposure to visible light play an important role in lowering activation barriers in the reaction between **6** and H₂O₂ to give CO. Overall, two reaction pathways have been identified for CO release from a 3-hydroxybenzo[g]quinolone.

 Received 11th October 2021
Accepted 27th December 2021

DOI: 10.1039/d1ra07527f

rsc.li/rsc-advances

Introduction

Organic carbon monoxide (CO)-releasing molecules are of current interest for use in evaluating the roles of CO in biological systems and as potential therapeutics.^{1,2} Of particular interest for biomedical applications are compounds that can be triggered so as to enable spatial and temporal control of CO release.^{3,4} Toward meeting this need, five general types of metal-free, visible-light induced CO releasing molecules have been reported (Scheme 1(a–e)).^{5–9} As a step toward advancing frameworks that are suitable for further applications (*e.g.*, for subcellular targeting), it is important to have a detailed mechanistic understanding of the CO release reaction of each motif.

Compound **1** (Scheme 1(a)) exhibits visible light-induced CO release at pH = 5.7–7.4 in its monoanionic form to give a single organic product.⁵ The overall yield for CO release from **1** has not been reported. ¹⁸O-labeling studies provide evidence that the carboxyl group is the source of the CO oxygen atom (C¹⁸O). A CO release reaction pathway involving a putative α -lactone

intermediate (Scheme 1(a), **1-int**) has been proposed for **1**. Notably, the CO release reaction of **1** is not affected by the presence of O₂, suggesting that the photoinduced pathway either does not involve a triplet state, or if present, its lifetime must be very short.

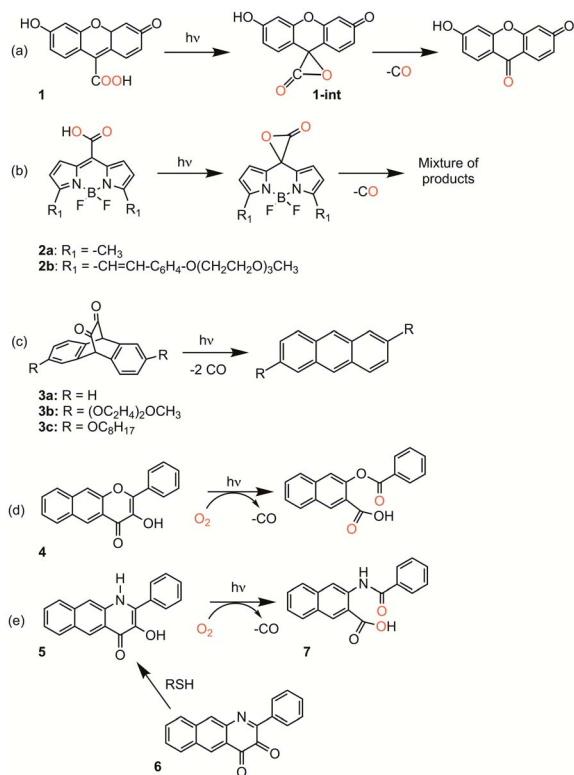
CO release from the BODIPY derivatives **2a** and **2b** (Scheme 1(b)) also occurs most readily from the monoanionic form, which is present at physiological pH.⁶ The overall yield of CO from **2b** is reduced from 87% to 45% in the presence of oxygen, suggesting the involvement of a triplet excited state in the reaction pathway. Transient absorption spectral features of **2a** and heavy atom-substituted analogs provide evidence that an excited state singlet is initially formed that undergoes rather inefficient intersystem crossing (ISC) to give a triplet state. From this triplet state, photoinduced electron transfer (PET) from the carboxylate to the BODIPY is proposed to give a triplet diradical species which undergoes ISC to give an α -lactone on the singlet energy surface. Release of CO from the α -lactone then occurs *via* non-photochemical fragmentation. Evidence for the proposed α -lactone intermediate in this system was put forth based on DFT studies involving a truncated analog.

The 1,2-diketone-type compounds **3a–3c** (Scheme 1(c)) undergo fast double decarbonylation, but only under conditions wherein water is excluded, as the formation of carbonyl hydrates prevents CO release.⁷ The CO release reaction from 1,2-

^aDepartment of Chemistry and Biochemistry, Utah State University, 0300 Old Main Hill, Logan, UT, 84322-0300, USA. E-mail: lisa.berreau@usu.edu

^bJerzy Haber Institute of Catalysis and Surface Chemistry, Polish Academy of Science, Niezapominajek 8, Krakow 30-239, Poland

 † Electronic supplementary information (ESI) available: ¹H NMR, mass spectrometry and UV-vis data. See DOI: 10.1039/d1ra07527f

Scheme 1 Metal-free CO releasing molecules. Red coloration indicates the results of ¹⁸O labelling studies.

diketones such as **3a–3c** occurs *via* Strating-Zwanenburg photodecarbonylation.^{10,11} This reaction occurs from both singlet and triplet manifolds *via* an initial step that involves either bond cleavage between a carbonyl and a methylene carbon, or homolytic cleavage between the carbonyl units, to give a diradical species. It is unclear whether CO release then occurs in a stepwise or concerted fashion, or whether 2 eq. CO or the CO dimer are initially released.¹¹

Our recent research has focused on investigations of the 3-hydroxybenzo[*g*]flavone framework **4** (Scheme 1(d)) as a light-triggered CO-releasing molecule.^{4,8,12,13} This compound exhibits quantitative CO release upon illumination with visible light ($\lambda_{\text{ill}} = 419$ nm). An ¹⁸O-labeling study showed quantitative incorporation of both atoms of ¹⁸O₂ into the depside product. Klán and coworkers performed additional mechanistic investigations of the O₂-dependent CO release reactivity of **4**.¹⁴ They identified three visible-light induced reaction pathways leading to CO release: (1) reaction of a neutral triplet excited state tautomer of **4** with ³O₂; (2) reaction of the ground state conjugate base of **4** with ¹O₂, which is produced *via* self-sensitization; and (3) inefficient photorearrangements of the triplet excited states of both **4** and its monoanion.

We recently reported light-induced CO delivery using the 3-hydroxybenzo[*g*]quinolone **5** (Scheme 1(e)).⁹ A key feature of **5** is its tight binding to bovine serum albumin protein ($K_a = 2.9 \times 10^6$) which is ~ 900 fold higher than that of **4** and enables the use of a protein:**5** complex for CO delivery to cells. Additionally, an oxidized prodrug form of this molecule (**6**, Scheme 1(e)), is

reduced by thiols, providing an approach toward activation in the reducing environment of some cancer cells. Use of the protein:**5** complex produced cytotoxicity values among the lowest reported to date for CO delivery to cancer cells. Additionally, the protein:**5** complex is the first CO delivery molecule to be reported to produce significant anti-inflammatory effects at nanomolar concentrations. Based on these results, and its non-toxic properties in cells, **5** is particularly attractive for further development as a light-triggered CO releasing molecule for biological and biomedical applications.

Herein we report combined experimental and computational studies of the mechanistic pathway of the visible light-induced CO release reaction of **5**. Interestingly, these studies revealed two pathways for CO release, with one pathway involving initial oxidation of the quinolone framework to **6** prior to CO release.

Materials and methods

Compounds **5** and **6** have been synthesized according to literature procedures.^{9,15} All other reagents were purchased from common vendors and used as received unless otherwise noted.

Physical methods

¹H NMR spectra were collected using a Bruker Avance III HD Ascend-500 spectrometer. UV-vis spectra were recorded at ambient temperature using a Cary 50Bio or a Hewlett-Packard 8453A diode array spectrophotometer. Fluorescence emission spectra were recorded using a Shimadzu RF-530XPC spectrometer using 1.0 cm quartz cells. The excitation and emission slit widths were set at 3.0 nm. Mass spectral data were collected at the Mass Spectrometry Facility, University of California, Riverside. CO gas was detected and quantified using an Agilent 3000A micro gas chromatograph with molecular sieve and Plot U columns and a thermal conductivity detector. H₂O₂ formation in the conversion of **5** to **6** was detected using commercial H₂O₂ test strips.

Computational methods

All computations were performed employing the ω B97XD¹⁶ exchange-correlation functional and the Def2-TZVP¹⁷ basis set. The only exception is ^{T1}TS_{OO}, which was fully optimized with the def2-SVP basis set, but despite many various attempts we were not able to re-optimize it with the def2-TZVP basis set. Hence, the activation energy connected with this transition structure was computed with the def2-TZVP basis using geometries of ^{T1}INT_{C2P} and ^{T1}TS_{OO} optimized with the def2-SVP basis set. Lowest lying triplet and broken symmetry singlet spin states were described with the unrestricted formalism. Excited singlet and triplet states were described with the TD-DFT¹⁸ method using a closed-shell ground state singlet as a reference. Minimum energy crossing points (MECP) between various potential energy surfaces (PESs) were optimized with the use of the meta-program crossing obtained courtesy of Prof. J. Harvey.¹⁹ The polarizable continuum model (PCM) using the integral equation formalism variant (IEFPCM) was used in all calculations to model the solvent (acetonitrile). All electronic



structure computations were done with the Gaussian 16 program.²⁰

Treatment of 6 with H₂O₂ (30%) in acetonitrile

H₂O₂ (30%, 5 μl) was added to a solution of 6 (1.5 × 10⁻⁴ M, 3 ml) in acetonitrile. The absorption spectral features of the solution were monitored in the absence or presence of illumination (419 nm). The same reaction under illumination conditions was also examined using ¹H NMR.

CO quantification from the reaction of 6 with H₂O₂

The diketone 6 (10⁻⁵ mol) was dissolved in acetonitrile (5 ml) in a 50 ml round bottom flask. Excess H₂O₂ (30%, 0.1 ml) was added and the flask was then sealed with a septum. The solution was stirred for 48 hours with or without illumination at 419 nm. A 10 ml sample of the headspace gas was used to determine the CO generated using gas chromatography. Approximately 0.6 eq. (illuminated) and 0.3 eq. of CO (non-illuminated), respectively, were produced. As a control for CO quantification under these conditions, light induced CO release from 4 produces 0.99 eq.

Results

Spectroscopic studies of the CO release reaction of 5

Illumination of a wet CH₃CN solution of 5 under aerobic conditions results in the formation of 7 (Scheme 1(e)) and the release of 0.90(2) eq. of CO as determined using ¹H NMR and gas chromatography. To gain further insight into this reaction, a solution of 5 in CD₃CN was illuminated using 419 nm light at ~35 °C and was monitored periodically using ¹H NMR as shown in Fig. 1. After 15 min of illumination (Fig. 1(b)), in addition to

starting material, two species are present, the CO release product 7 and the diketone 6 (Scheme 1(e)).¹⁵ The formation of the diketone 6 indicates that upon illumination at least some of the reactant (5) undergoes two-electron oxidation with the release of H₂O₂. The formation of H₂O₂ was confirmed by examining the reaction mixture using H₂O₂ test strips (Fig. S1†) which turned blue indicating formation of a peroxide species. We note that an analogous experiment involving illumination of the extended flavonol 4 did not produce the change in the peroxide strip color (Fig. S1†), indicating the unique formation of H₂O₂ in the illumination of 5. Continuing with the reaction of 5, after 30 min (Fig. 1(c)), the ¹H NMR resonances associated with the starting material 5 are gone, and only the resonances for 6 and the carboxylic acid-containing CO release product 7 remain. After 2 h the integrated intensity for the signals for 6 diminished further while those of 7 increased suggesting a second reaction pathway wherein 6 may react with H₂O₂ to give 7. Notably, use of ¹⁸O₂ in the reaction results in quantitative incorporation of two labelled oxygen atoms in 7 (Fig. S2†). This provides evidence that the reaction pathway involving 6 results in the incorporation of labelled oxygen atoms derived from O₂. Illumination of 5 using 465 nm lamps produces similar results (Fig. S3†). A mixture of 6 and 7 is formed in the first few hours of illumination followed by the disappearance of the resonances associated with 6 at long illumination times (24 h) to give resonances only associated with 7.

The visible light-induced CO release reaction of 5 (at 419 nm) in wet acetonitrile was also monitored using UV-vis absorption spectroscopy. As shown in Fig. 2, loss of the absorption features of 5 over the first ~12 min of illumination coincides with the appearance of a new broad absorption band at ~480 nm, which is consistent with the formation of a substoichiometric amount of the diketone 6 based on the individual absorption spectral

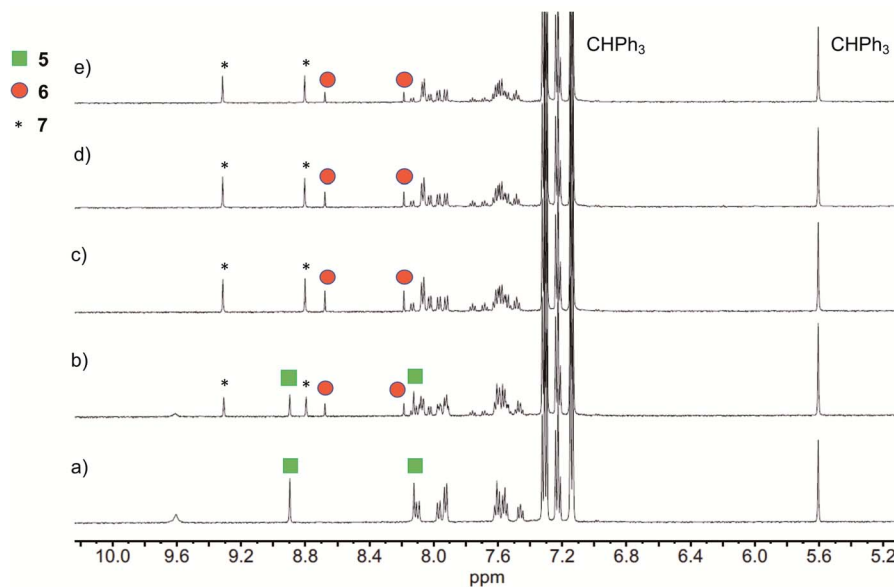


Fig. 1 ¹H NMR features of a solution of 5 in wet CD₃CN with illumination (419 nm) at ~35 °C under O₂: (a) Prior to illumination; (b) 15 min; (c) 30 min; (d) 1 h and (e) 2 h. The combined integrations of the indicated resonances of 5, 6 and 7 are consistent versus the internal standard CHPh₃ over the course of illumination.



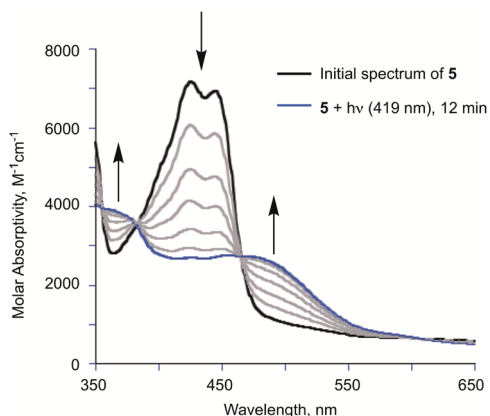


Fig. 2 Changes in the absorption spectrum of 5 in acetonitrile upon illumination with 419 nm light.

features of the compounds.⁹ Two isosbestic points at ~ 380 and 465 nm suggest clean conversion of 5 to 6. After ~ 20 min of growth of the band at ~ 480 nm, this feature begins to decay.

Reactivity of 6 with H₂O₂

To evaluate the reactivity of 6 with H₂O₂, independent experiments were performed. Treatment of the diketone 6 dissolved in acetonitrile with excess aqueous H₂O₂ (30%) under ambient conditions results in the disappearance of its absorption band at 480 nm over 8 h in absence of illumination and within 45 min with illumination at 419 nm (Fig. 3(a) and (b), respectively). Compound 7 is formed in the illuminated sample as determined by ¹H NMR (Fig. S4[†]). CO gas is generated under both thermal and illuminated conditions (~ 0.3 and 0.6 eq., respectively). The low amount of CO generated under these conditions may be due to hydration of the diketone or other water-dependent decomposition pathways as 6 undergoes spectroscopic changes in the presence of added D₂O to produce unidentified species (Fig. S5[†]).

Based on these investigations, we hypothesized that the light-driven CO release reactivity of 5 to produce 7 could be proceeding *via* at least two light-driven pathways. The primary pathway could be similar to those of 4¹⁴ and 3-hydroxyflavone.^{21,22} These previously reported pathways involve excited

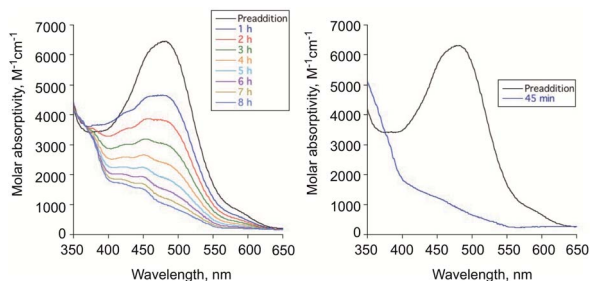


Fig. 3 Absorption spectral features for 6 prior to and following addition of H₂O₂ (30%) under thermal (left) and illumination conditions (right). The decay of the absorption band for 6 occurs over 8 h under thermal conditions and in under an hour under illumination (419 nm).

state proton-transfer tautomer triplet state reactivity with triplet oxygen. The reaction of 5 with O₂ that leads to formation of diketone 6 and H₂O₂, which then appears to subsequently undergo reaction leading to CO release, has not been previously reported for a quinolone compound. To gain further insight into the visible-light induced CO release pathways involving 5, we turned to DFT calculations.

Computational studies; low-lying excited states of 5

TD-DFT results indicate that the first excited singlet state and two lowest lying triplet states of 5 originate from one electron excitations within four frontier molecular orbitals (HOMO-1, HOMO, LUMO and LUMO+1), whose contours are shown in Fig. 4. In the S₁ and T₁ states the HOMO \rightarrow LUMO excitation is the leading one, whereas in the T₂ state the two major excitations are HOMO-1 \rightarrow LUMO and HOMO \rightarrow LUMO+1.

Tautomeric forms with a proton located on the C3- or C4-bound oxygen atoms, which are labelled with 5 and 5a, respectively, differ in relative stability depending on the nature of the excited state. For the S₁ and T₁ states the ^{S1}5a and ^{T1}5a forms are the most stable, whereas for the S₀ and T₂ states the ^{S0}5 and ^{T2}5 forms are the lower energy ones (Fig. 5). Adiabatic barriers computed for the proton transfer steps (5 \rightarrow TS_{PT} \rightarrow 5a) are rather low, *i.e.* amount to 14.2, 5.0, 3.0 and 9.9 kcal mol⁻¹ for S₀, S₁, T₁ and T₂ potential energy surfaces (PESS), respectively. For the ^{S1}5 species one can envisage several potential channels for its decay. First, an internal conversion process, *i.e.* S₁ \rightarrow S₀, may lead to de-excitation and dissipation of the excess energy. Second, an intersystem crossing may lead to the triplet manifold. Interestingly, a direct transition from S₁ to T₁ is not an easy process. For the tautomer 5 we could not locate a minimum energy crossing point (MECP) between ^{S1}5 and ^{T1}5, most likely due to the fact that S₁ and T₁ have PESSs of very similar shape. For the tautomer 5a the optimized crossing point (^{S1-T1}MECP2) is quite high in energy, *i.e.* it is 16.4 kcal mol⁻¹ higher than ^{S1}5a (Fig. 5), which suggests this reaction channel is rather unlikely. On the other hand, MECPs between the S₁ and T₂ states have energies only slightly higher than the two minima on the S₁ PES, *i.e.* by 3.9 and 0.3 kcal mol⁻¹ for ^{S1-T2}MECP1 and ^{S1-T2}MECP2, respectively, and hence, they are the most likely gates to the triplet manifold. Importantly, the T₂ state lies lower in energy than S₁ and it

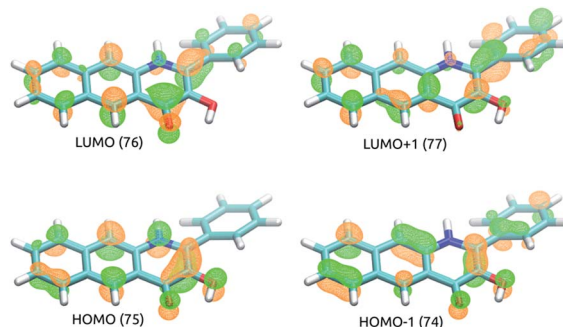


Fig. 4 Contours of frontier molecular orbitals of 5.



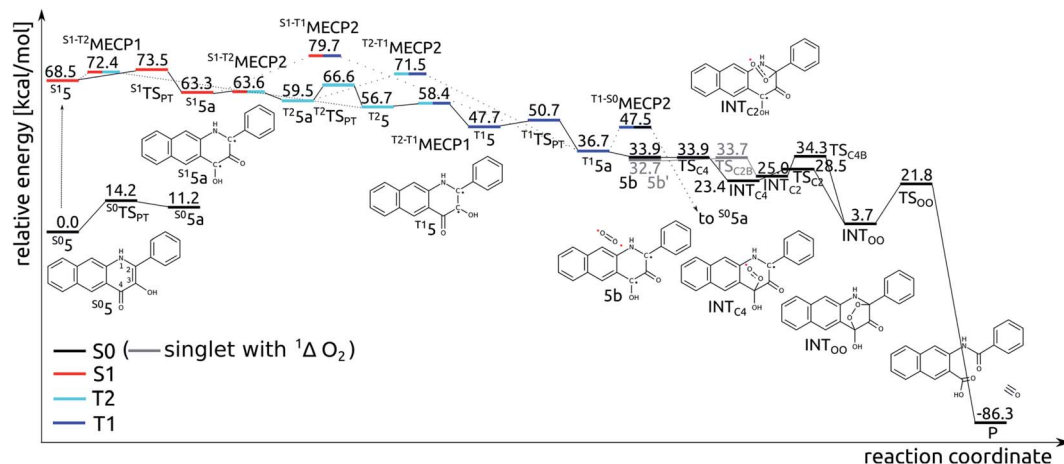


Fig. 5 Relative energy of species in the calculated light-induced reaction pathway of 5 with O₂.

features a low lying MECP with the T1 state, ^{T2-T1}MECP1, which lies only 1.7 kcal mol⁻¹ higher than ^{T2}5. Hence, it is suggested that the lowest lying triplet state is populated through a sequence of steps encompassing proton transfer on the S1 PES (^{S1}5 → ^{S1}5a), intersystem crossing to the T2 state (^{S1}5a → ^{T2}5a), another proton transfer step (^{T2}5a → ^{T2}5) and finally an internal conversion from T2 to T1 (^{T2}5 → ^{T1}5). The ^{T1}5a form, easily formed *via* proton transfer ^{T1}5 → ^{T1}5a, is the lowest energy excited state species which is supposed to live long enough to have a chance to react with the triplet dioxygen, as described in the following subsections. Indeed, the optimized minimum energy crossing point between T1 and S0, *i.e.* ^{T1-S0}MECP2, lies 10.8 kcal mol⁻¹ above the ^{T1}5a minimum, which should lend this triplet species substantial lifetime.

Addition of O₂ to ^{T1}5a

The ^{T1}5a species forms an encounter complex with triplet dioxygen and two electronic states are almost degenerate for this complex. First, the unpaired electrons of the two triplet

entities are coupled to a (broken symmetry) singlet spin state (**5b**; for spin density plots see Fig. 6). Second, the organic molecule returns to its ground closed-shell singlet state while dioxygen is excited to the ¹Δ_g singlet state (**5b'**). The two states are computed to be only 1.2 kcal mol⁻¹ apart and both are very reactive towards C–O bond formation. Irrespective of the electronic state of the encounter complex, O₂ addition to the organic molecule is a stepwise process, whereby the two C–O bonds are formed in two successive elementary reactions. The computed barriers for binding of O₂ at C2 (**5b** → INT_{C2}) is only 1.0 kcal mol⁻¹, whereas the barrier for attack of triplet O₂ on C4 (**5b** → INT_{C4}) vanishes completely. Spin density maps computed for resulting intermediates (INT_{C2} and INT_{C4}; Fig. 6) indicate that the binding process engages one pair of electrons with anti-parallel spins, whereas the other two electrons remain localized on O₂^{••} and the ring. The latter couple to a bonding pair when the second C–O bond forms yielding the endoperoxide intermediate INT_{OO}. The decay of INT_{OO} with the release of CO is a symmetry allowed reaction, which involves concerted and synchronous cleavage of two C–C and one O–O bonds.²³ This reaction pathway is similar to those reported for **4**¹⁴ and 3-hydroxyflavone.^{21,22}

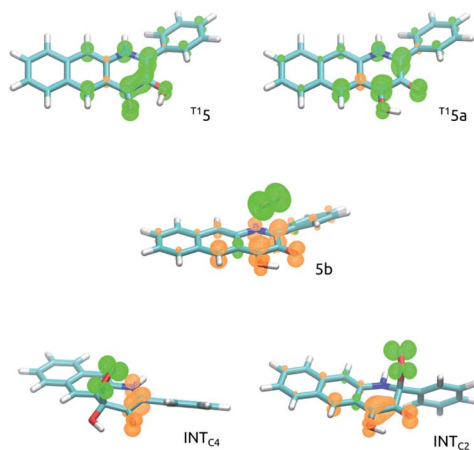


Fig. 6 Spin density maps of intermediates involved in C–O bond formation in the reaction of 5 with O₂.

Reaction of ^{T1}5a with O₂ leading to **6** and H₂O₂

The experimental results described above strongly suggest that in the photoreaction of 5 with O₂ the diketone **6** and H₂O₂ are also formed. Insights into how this process might proceed were obtained *via* DFT calculations, with the results summarized in Fig. 7. First, the singlet encounter complex between ^{T1}5a and ³O₂ with O₂ bound close to C4–OH (**5c**) forms. Its energy is only slightly higher (by 0.3 kcal mol⁻¹) than for **5b**. Second, formal hydrogen atom transfer from the phenolic oxygen to O₂ leads to a significantly more stable diradical species INT_{HOO}. The detailed mechanism of this step is most likely beyond the reach of DFT single determinant methods. Multiple attempts to locate a TS on the open-shell singlet PES failed, as the triplet converges to closed-shell ^{S0}5a and ³O₂, whereas the reaction might proceed on the open-shell triplet PES. Then, the peroxy radical



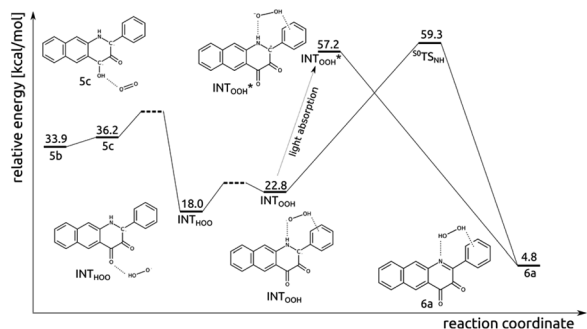


Fig. 7 Relative energy of species in the light-induced reaction pathway of **5** with O_2 to form **6a**.

migrates and forms H-bonding contacts with N1-H and the phenyl substituent. The INT_{HOO} to INT_{OOH} step is endoenergetic by $4.8 \text{ kcal mol}^{-1}$. The transition state for the direct hydrogen atom transfer from N1 to OOH was optimized ($^S0TS_{NH}$), however its energy is very high ($41.6 \text{ kcal mol}^{-1}$ higher than for INT_{HOO}), which renders this process very unlikely. However, a charge-transfer excitation within the singlet manifold leads to the closed-shell singlet species INT_{OOH}^* , which relaxes with no additional barriers directly to species **6a**.

Thermal reaction between diketone (**6**) and H_2O_2

Compound **6** and H_2O_2 form an encounter complex **6a** that is stabilized by a hydrogen bond between H_2O_2 and the C4-bound oxygen. Two reaction channels lead from **6a** to INT_{OO} , one through INT_{C2P} and the second through INT_{C4P} (Fig. 8). To form either of them a proton needs to be transferred from the oxygen atom, which forms a bond with the respective carbon atom (C2 or C4), to N1 or O bound to C4. Simultaneous proton transfer and formation of the C–O bond proceed through a strained transition structure featuring a four-membered ring. In consequence, the computed barriers are very high, *i.e.* 37.3 and $38.8 \text{ kcal mol}^{-1}$ for $6a \rightarrow TS_{C2P} \rightarrow INT_{C2P}$ and $6a \rightarrow TS_{C4P} \rightarrow INT_{C4P}$, respectively. When a single water molecule acts as

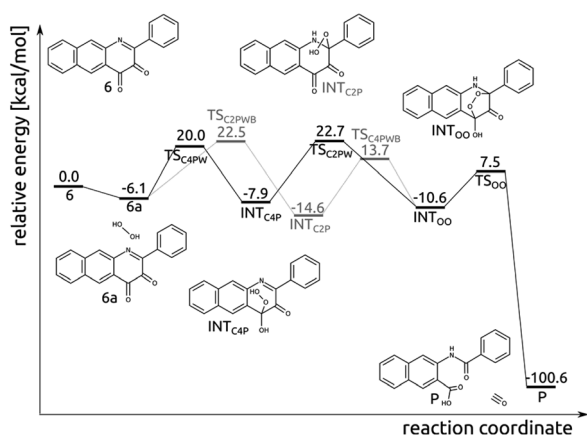


Fig. 8 Relative energy of species in the thermal reaction pathway of **6** with H_2O_2 .

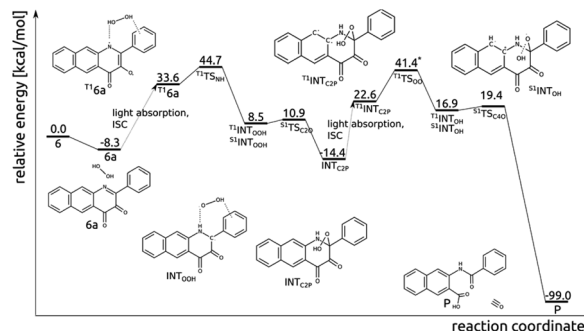


Fig. 9 Relative energy of species in the visible light-induced reaction pathway of **6** with H_2O_2 . *The relative energy with respect to $^T1INT_{C2P}$ was computed for geometries optimized with the def2-SVP basis set.

a catalyst and mediates the proton transfer, then the barriers drop significantly, to 28.6 and 26.1 for TS_{C2PW} and TS_{C4PW} , respectively (Fig. 8). Similarly, the subsequent step whereby the second C–O bond is formed was modelled with a single water molecule as a catalyst. As it is hard to estimate how many water molecules might be available in the vicinity of the encounter complex **6a**, the barriers computed here for the two channels leading from **6a** to INT_{OO} are to be considered only as qualitative, as they merely show that water can facilitate the process.

Photo-induced reaction between diketone (**6**) and H_2O_2

Excitation of the encounter complex **6a** to the lowest lying triplet state (T1_6a), *via* singlet excitation and subsequent intersystem crossing, opens an efficient route for hydrogen transfer from H_2O_2 to N1 and subsequent formation of the C2–OOH bond (Fig. 9). In the triplet state N1 has significant radical character, which renders the H-atom transfer process to be fairly easy; $^T1TS_{NH}$ is coupled with a barrier of $10.9 \text{ kcal mol}^{-1}$. In the resulting intermediate INT_{OOH} unpaired electrons are located on HOO and semiquinone radicals and triplet and open-shell singlet spin states are degenerate. Coupling of these radicals in the singlet state requires overcoming a tiny barrier and leads to the closed-shell intermediate INT_{C2P} , encountered already in the thermal reaction between **6** and H_2O_2 . Excitation of INT_{C2P} to the lowest lying triplet state provides a feasible route for O–O bond cleavage and subsequent release of CO. In the triplet spin state, the aromatic ring can quite easily provide the OOH moiety with one electron, *i.e.* with barrier of $23.4 \text{ kcal mol}^{-1}$ connected with $^T1TS_{OO}$, which aids O–OH bond cleavage. In the resulting intermediate INT_{OH} the two unpaired electrons are again considerably separated, and triplet and singlet spin state are energetically degenerate. In the singlet state attack of the HO^- group on C4 is very easy ($^S1TS_{C4O}$, barrier of $2.2 \text{ kcal mol}^{-1}$) and leads directly to the depside product and CO.

Discussion and conclusions

The structurally similar 3-hydroxyflavone (3-HfH) and 3-hydroxyquinolone (3-HqH) are substrates for enzyme-catalyzed dioxygenase-type CO release reactions in bacteria and fungi.^{24,25} Compounds of this type have also been shown to



undergo O_2 -dependent, UV-light-induced CO release. For example, 3-HfIH undergoes incorporation of both atoms of O_2 and expulsion of CO in the presence of a photosensitizer (e.g., Rose Bengal).²⁶ In this reaction, 1O_2 reacts with the ground state form of 3-HfIH in a [3 + 2] cycloaddition to form a cyclic peroxide from which cleavage of two carbon-carbon bonds results CO release. In the absence of a photosensitizer, UV-light illumination has been proposed to result in the formation of an excited state triplet tautomeric form of 3-HfIH, which then directly reacts with 3O_2 .²¹

We are investigating the visible light induced CO release properties of structural analogs of 3HfIH and 3HqH with extended conjugation (Scheme 1(d and e)).^{4,8,9,12,13} Notably, the 3-hydroxybenzo[g]quinolone **5** (Scheme 1(e)) binds tightly to bovine serum albumin which enables protein delivery of this CO releasing molecule to cancer cells. Visible light-induced CO release from the 5:albumin complex produces anti-cancer and potent anti-inflammatory effects.⁹

In this contribution we report spectroscopic and computational studies of the visible light-induced CO release reaction of **5** under aerobic conditions. Notably, in addition to the observed formation of the CO release depside product **7**, the diketone **6** is identifiable in the reaction mixture. Over the course of illumination, **6** disappears from the reaction mixture. Independent studies show that **6** undergoes reaction with aqueous H_2O_2 to give **7** and CO. DFT studies of the direct reaction of **5** with O_2 provide evidence for a light-driven CO release pathway (Path A, Scheme 2) that is akin to that previously described for 3-HfIH derivatives.^{21,22} Formation of an excited triplet tautomer enables reactivity with 3O_2 resulting in C-C and C-O bond cleavage yielding CO and depside.

The formation of **6** and H_2O_2 in the light-induced reaction of **5** is supported by DFT studies which provide initial insight into how these species can be generated (Fig. 7; Path B Scheme 2). Subsequent thermal reactivity between the diketone **6** and H_2O_2 appears to be feasible only in the presence of water, which lowers the activation barriers for C-O bond formation. The reaction between the diketone **6** and H_2O_2 to release CO is facilitated by excitation to the lowest triplet state. These combined results suggest that CO release *via* reaction of the diketone **6** with H_2O_2 likely proceeds *via* a light-driven process. The evidence provided herein suggests that this CO release

reaction is less efficient, possibly due to decomposition pathways for the diketone involving water.

Quinolones are of current interest as anticancer compounds.^{27,28} The H_2O_2 induced CO release reactivity of **6** under illumination conditions is of interest in relation to the role that H_2O_2 is suggested to have in promoting tumor proliferation.²⁹ Diketone molecules such as **6** may offer an approach toward reducing H_2O_2 levels in combination with CO delivery to produce anti-cancer effects. Our ongoing work is focused on advancing light-driven CO delivery using extended quinolones and their oxidized diketone forms, which are families of heterocyclic compounds that have received minimal attention to date.^{9,15}

Data availability

Optimized structures were deposited in the ioChem-BD repository. See DOI: 10.19061/iochem-bd-4-32.

Author contributions

MP, TB and LMB conceptualized the project; MP, TB, JGDE, and CTD performed the experimental investigations; MP, TB and LMB wrote the manuscript.

Conflicts of interest

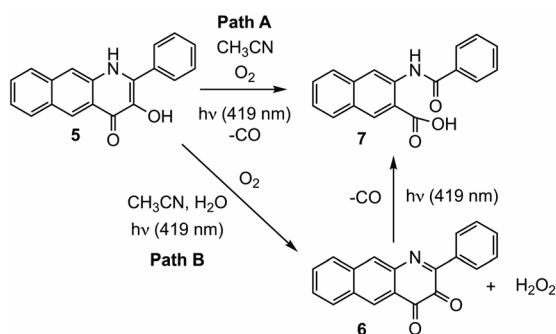
There are no conflicts to declare.

Acknowledgements

We thank the NIH (R15GM124596 to L. M. B.) and the NSF (CHE-1429195 for Brüker Avance III HD Ascend-500 spectrometer). This research was supported in part by PL-Grid Infrastructure. Computations were performed in the AGH Cyfronet Supercomputer Centre. T. B. acknowledges partial financial support of the project by the statutory research fund of ICSC PAS.

References

- 1 T. Slanina and P. Šebej, *Photochem. Photobiol. Sci.*, 2018, **17**, 692–710.
- 2 N. Abeyrathna, K. Washington, C. Bashur and Y. Liao, *Org. Biomol. Chem.*, 2017, **15**, 8692–8699.
- 3 M. Kourti, W. G. Jiang and J. Cai, *Oxid. Med. Cell. Longevity*, 2017, 9326454.
- 4 L. S. Lazarus, A. D. Benninghoff and L. M. Berreau, *Acc. Chem. Res.*, 2020, **53**, 2273–2285.
- 5 L. A. Antony, T. Slanina, P. Šebej, T. Šolomek and P. Klán, *Org. Lett.*, 2013, **15**, 4552–4555.
- 6 E. Palao, T. Slanina, L. Muchová, T. Šolomek, L. Vítek and P. Klán, *J. Am. Chem. Soc.*, 2016, **138**, 126–133.
- 7 P. Peng, C. Wang, Z. Shi, V. K. Johns, L. Ma, J. Oyer, A. Copik, R. Igarashi and Y. Liao, *Org. Biomol. Chem.*, 2013, **11**, 6671–6674.



Scheme 2 Reaction pathways leading to CO release from **5** under visible light illumination.



- 8 S. N. Anderson, J. M. Richards, H. J. Esquer, A. D. Benninghoff, A. M. Arif and L. M. Berreau, *ChemistryOpen*, 2015, **4**, 590–594.
- 9 M. Popova, L. S. Lazarus, S. Ayad, A. D. Benninghoff and L. M. Berreau, *J. Am. Chem. Soc.*, 2018, **140**, 9721–9729.
- 10 J. Strating, B. Zwanenburg, A. Wagenaar and A. C. Udding, *Tetrahedron Lett.*, 1969, **10**, 125–128.
- 11 R. Mondal, A. N. Okhrimenko, B. K. Shah and D. C. Neckers, *J. Phys. Chem. B*, 2008, **112**, 11–15.
- 12 L. S. Lazarus, H. J. Esquer, A. D. Benninghoff and L. M. Berreau, *J. Am. Chem. Soc.*, 2017, **139**, 9435–9438.
- 13 M. Popova, T. Soboleva, A. M. Arif and L. M. Berreau, *RSC Adv.*, 2017, **7**, 21997–22007.
- 14 M. Russo, P. Štacko, D. Nachtigallová and P. Klán, *J. Org. Chem.*, 2020, **85**, 3527–3537.
- 15 M. D. Bilokin, V. V. Shvadchak, D. A. Yushchenko, A. S. Klymchenko, G. Duportail, Y. Mely and V. G. Pivovarenko, *Tetrahedron Lett.*, 2009, **50**, 4714–4719.
- 16 J.-D. Chai and M. Head-Gordon, *Phys. Chem. Chem. Phys.*, 2008, **10**, 6615–6620.
- 17 F. Weigend and R. Ahlrichs, *Phys. Chem. Chem. Phys.*, 2005, **7**, 3297–3305.
- 18 R. Bauernschmitt and R. Ahlrichs, *Chem. Phys. Lett.*, 1996, **256**, 454–464.
- 19 J. N. Harvey, M. Aschi, H. Schwarz and W. Koch, *Theor. Chem. Acc.*, 1998, **99**, 95–99.
- 20 M. J. Frisch, G. W. Trucks, H. B. Schlegel, G. E. Scuseria, M. A. Robb, J. R. Cheeseman, G. Scalmani, V. Barone, G. A. Petersson, H. Nakatsuji, X. Li, M. Caricato, A. V. Marenich, J. Bloino, B. G. Janesko, R. Gomperts, B. Mennucci, H. P. Hratchian, J. V. Ortiz, A. F. Izmaylov, J. L. Sonnenberg, D. Williams-Young, F. Ding, F. Lipparini, F. Egidi, J. Goings, B. Peng, A. Petrone, T. Henderson, D. Ranasinghe, V. G. Zakrzewski, J. Gao, N. Rega, G. Zheng, W. Liang, M. Hada, M. Ehara, K. Toyota, R. Fukuda, J. Hasegawa, M. Ishida, T. Nakajima, Y. Honda, O. Kitao, H. Nakai, T. Vreven, K. Throssell, J. A. Montgomery Jr, J. E. Peralta, F. Ogliaro, M. J. Bearpark, J. J. Heyd, E. N. Brothers, K. N. Kudin, V. N. Staroverov, T. A. Keith, R. Kobayashi, J. Normand, K. Raghavachari, A. P. Rendell, J. C. Burant, S. S. Iyengar, J. Tomasi, M. Cossi, J. M. Millam, M. Klene, C. Adamo, R. Cammi, J. W. Ochterski, R. L. Martin, K. Morokuma, O. Farkas, J. B. Foresman, and D. J. Fox, *Gaussian 16, Revision A.03*, Gaussian, Inc., Wallingford CT, 2016.
- 21 S. L. Studer, W. E. Brewer, M. L. Martinez and P.-T. Chou, *J. Am. Chem. Soc.*, 1989, **111**, 7643–7644.
- 22 Z. Szakács, M. Bojtár, L. Drahos, D. Hessz, M. Kállay, T. Vidóczy, I. Bitter and M. Kubinyi, *Photochem. Photobiol. Sci.*, 2016, **15**, 219–227.
- 23 A. M. Miłaczewska, E. Kot, J. A. Amaya, T. M. Makris, M. Zajac, J. Korecki, A. Chumakov, B. Trzewik, S. Kędracka-Krok, W. Minor, M. Chruszcz and T. Borowski, *Chem.–Eur. J.*, 2018, **24**, 5225–5237.
- 24 S. Fetzner, *Appl. Environ. Microbiol.*, 2012, **78**, 2505–2514.
- 25 U. Frerichs-Deeken, K. Rangelova, R. Kappl, J. Hüttermann and S. Fetzner, *Biochemistry*, 2004, **43**, 14485–14499.
- 26 T. Matsuura, H. Matsushima and R. Nakashima, *Tetrahedron*, 1970, **26**, 435–443.
- 27 J. Rehulka, K. Vychodilova, P. Kejci, S. Gurska, P. Hradil, M. Hajduch, P. Dzubak and J. Hlavac, *Eur. J. Med. Chem.*, 2020, **192**, 112176.
- 28 K. Burglová, G. Rylová, A. Markos, H. Prichystalova, M. Sural, M. Petracek, M. Medvedikova, G. Tejral, B. Sopko, P. Hradil, P. Dzubak, M. Hajduch and J. Hlavac, *J. Med. Chem.*, 2018, **21**, 3027–3036.
- 29 C. Hegedus, K. Kovács, Z. Polgár, Z. Regdon, E. Szabó, A. Robaszkievicz, H. J. Forman, A. Martner and L. Virág, *Redox Biol.*, 2018, **16**, 59–74.

